Int. J. Electrochem. Sci., 15 **(2020)** 3825 – 3835, doi: 10.20964/2020.05.51

International Journal of
ELECTROCHEMICAL
SCIENCE
www.electrochemsci.org

Short Communication

Effect of Marble Dust and Silica Fume admixtures replaced in ordinary Portland cement on corrosion behavior of carbon steel in the concrete after exposure to 5 wt% NaCl solution

Shengpin Liu[1], *Wu Zhao*[2,*]

[1] School of Architecture and Urban planning , Shandong Jianzhu University, Jinan, 250100 ,China
[2] College of Water Conservancy and Civil Engineering, Shandong Agriculture University, Tai'an 271000, China
[*]E-mail: wuzhao@sdau.edu.cn, wuzhao_2000@163.com

Received: 5 January 2020 / *Accepted:* 20 February 2020 / *Published:* 10 April 2020

Recent studies show that corrosion resistivity of reinforced concrete can be enhanced by modifying the structure of concrete, especially cement replacement by mineral admixtures. In this work, the effect of partial replacement of ordinary Portland cement (OPC) on corrosion behavior of carbon steel reinforced concrete in 5 wt% NaCl solution were investigated. The OPC was partially replaced by a combination of marble dust (MD) and silica fume (SF) admixtures. Potentiodynamic polarisation measurement, electrochemical impedance spectroscopy, cyclic voltammetry and water absorption test were used to evaluate the corrosion behavior of carbon steel rebar. The electrochemical results showed that the sample with MD (30 kg/m^3) and SF (30 kg/m^3) cement replacement had higher corrosion resistance and potential than all the others. The absorption results revealed that the SF30MD30 sample significantly changed the water absorption of reinforced concrete. The scanning electron microscopy images of carbon steel surface showed that low corrosion products and narrow pits appeared on the surface of SF30MD30 sample which was in accordance with the results obtained from electrochemical experiments. These findings indicated that mineral admixtures had resulted in a reduction of hydroxide ion concentrations which had led to an increase in passivation of the reinforcement steel and an improved corrosion resistance.

Keywords: Corrosion resistance; Marble dust and silica fume admixtures; Ordinary Portland cement; carbon steel rebar; Electrochemical technique; Water absorption

1. INTRODUCTION

Recent studies show that corrosion of reinforced concrete can be decreased by increasing the strength of the concrete, especially in chloride contaminated media [1]. Reinforced concrete needs steel bars to provide the tensile strength required in structural concrete [2]. However, when steel bars become corroded, due to the rust formation on the surface of the bar, the bond between the concrete and the steel bar is destroyed [3]. Concrete permeability is an essential feature for the durability of concrete as it transfers easily water or other liquids through the concrete and subsequently transmits corrosive materials [4].

In the past decades, different types of waste materials, for example marble waste dust, metallic based furnace slag, tire rubbers, lime stone, fly ash and silica fume (SF), have been frequently used in concrete structures [5-9]. Previous researches had revealed that these waste materials can improve concrete structures properties, specifically its durability, workability and compressive strength in the concrete production. Ergün's study exhibited that using waste marble dust (MD) (5.0% and 7.5%) as partial cement replacement resulted in an enhanced compressive strength [10]. Aliabdo et al. investigated the effect of waste MD on mechanical properties of concrete at different mass [11]. The results indicated that the use of waste MD as a partial sand replacement develops the mechanical properties in concrete, mainly because of a filler effect.

Furthermore, the use of SF in concrete can be beneficial in reducing corrosion rate [12]. Recent studies showed that silicate compositions can significantly reduce the penetration and the mobility of chloride ions in concrete structures [13, 14]. Kulakowski et al. indicated the effect of SF additions on the corrosion behavior of reinforced concrete by changing their concentration [15]. When SF concentration was greater than 10%, the corrosion potential of carbonation-induced reinforcement increased. The use of micro and nanotechnology in building materials has increased the metal's corrosion resistance and optimized the electrochemical, physical and chemical properties of the structures [16]. Feky et al. revealed the corrosion resistance of steel rebar was increased with the increase in nano-silica/potassium silicate ratios which can be related to the size of nano-silica particles and the ability to fill the pores in potassium silicate coating [17].

In this research, an investigation on corrosion resistance of the steel rebar embedded in blended concrete under different concentrations of SF and MD was done. The electrochemical impedance spectroscopy technique was applied to study the corrosion properties of the samples in 5 wt% NaCl solution.

2. MATERIALS AND METHOD

In this study, concrete was prepared at room temperature under controlled conditions using ordinary Portland cement (OPC), fine, coarse aggregates and water. The chemical composition of cement is presented in Table 1. The cement replacement were done with silicon fume (SF), marble dust (MD) and combination of the two. The binder content of the mixtures was 400 kg/m^3. The water to cement ratio of the mixtures was 0.5.

Table 2 indicate the composition of the different mixtures. The prepared mixes were poured into the cylinder molds with 10 cm diameter and 30 cm height at room temperature with 90% relative humidity for one day. The specimens were cast and then demolded after 24 hours. In order to consider the effect of incorporations of SF and MD on corrosion behavior of the reinforced concretes, electrochemical experiments were done on Q235 carbon steel rebar in 5 wt% NaCl solution as an aggressive environment for 2 months. The composition of the Q235 carbon steel rebar is indicated in Table 3.

Table 1. Chemical composition of the silica fume and marble dusts

	Ordinary Portland cement (wt%)	Silica fume (wt%)	Marble dust (wt%)
SiO_2	20.55	87.74	1.4
Al_2O_3	4.67	0.00	0.7
Fe_2O_3	3.05	0.98	0.4
CaO	64.15	2.34	84.6
MgO	2.06	6.53	0.6
K_2O	0.67	3.13	0.1
Na_2O	0.24	1.58	0.1
SO_3	2.93	2.78	0.3
LOI	0.87	6.28	2.4

Table 2. Composition of reinforced concrete mixture (kg/m^3)

Mix no.	Ordinary Portland cement	Silica fume	Marble dust	Water	Fine aggregates	Coarse aggregates
1 (OPC)	400	0	0	200	710	1025
2 (SF60MD0)	340	60	0	200	695	990
3 (SF0MD60)	340	0	60	200	695	990
4 (SF30MD30)	340	30	30	200	695	990

Table 3. The composition of the Q235 carbon steel rebar (wt%)

Carbon	Mn	Si	P	S	Cr	Ni	Fe
0.17	0.45	0.26	0.0047	0.017	0.15	0.10	Residual

Electrochemical impedance spectroscopy (EIS) was used for electrochemical analysis of the samples. A conventional three-electrode cell was applied for the measurements which contain the steel rebar embedded in concrete as working electrode, a platinum wire as a counter electrode and a saturated calomel electrode as the reference electrode. The EIS analysis was carried out in a frequency range of 10 mHz to 0.1 MHz. The potentiodynamic polarization (CorrTest Instruments Corp., Ltd., China) measurement was conducted from 0.25V at 1 mV/s scanning rate. The cyclic voltammetry analysis was carried out between -1.5V and 1.5 V at scan rate with 50 mV/s and recorded sixth cyclic voltammograms for comparison between samples. According to ASTM C642, water absorption value was determined by drying a sample with a constant mass, and then immersing it in water and measuring the mass of saturated surface dry. The water absorption was the proportion of the difference between the two values measured to the dry mass.

3. RESULTS AND DISCUSSION

Figure 1 shows polarization curves of carbon steel rebar in different concrete samples exposed to 5 wt% NaCl solution after two months exposure time. As shown in fig. 1, the anodic polarization curves are investigated by passive zones at all reinforcing steels, showing that the passive layers have clearly formed on the surface of steel once they are exposed to the marine environment [18]. Moreover, a significant shift is observed in corrosion potential to a positive direction which reveals that the dissolution of anodic metal was effectively retarded by changing the concrete content [19, 20].

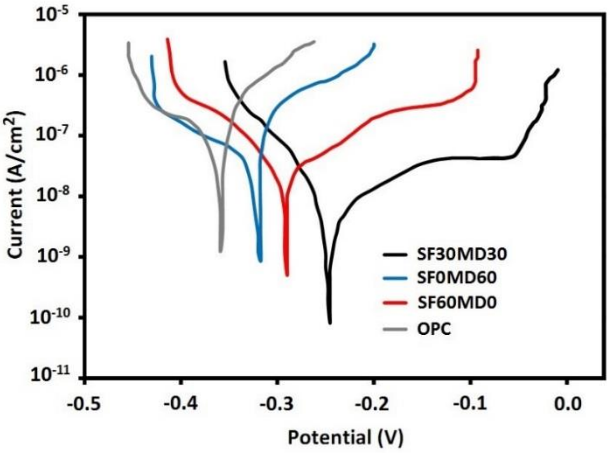

Figure 1. Potentiodynamic polarisation of carbon steel embedded in different concrete samples exposed to 5 wt% NaCl solution after two months exposure time

Table 4. Corrosion current density and corrosion potential of the carbon steel rebars

Mixtures	Corrosion current density	Corrosion potential	β_c	$-\beta_a$
OPC	0.343 μA/cm^2	-0.372 V	52 mVdec^{-1}	23 mVdec^{-1}
SF60MD0	0.076 μA/cm^2	-0.285 V	57 mVdec^{-1}	32 mVdec^{-1}
SF0MD60	0.091 μA/cm^2	-0.323 V	56 mVdec^{-1}	27 mVdec^{-1}
SF30MD30	0.032 μA/cm^2	-0.247 V	53 mVdec^{-1}	35 mVdec^{-1}

Compared to all samples, the passive region was much wider at the SF30MD30 sample, and the passive current density was lower than that of the other specimens, showing the corrosion resistance of the passivated steel was enhanced for SF30MD30 sample. More corrosion resistance in the SF30MD30 sample can be associated to the SF that reacted with released calcium hydroxide during the cement hydration and forms additional calcium silicate hydrate, which improved the mechanical

properties and durability of the concrete [23]. The values of corrosion current density and corrosion potential are indicated in table 4 which is achieved from the polarization diagrams in Figure 1.
The level of corrosion can be defined in four levels provided by the Durar Network Specification [21]. However, the corrosion current density of SF30M30 sample in 5 wt% NaCl environment was lower than that of the other specimens (Table 4). Thus, except the OPC sample, all steel reinforced concretes stayed in the passive state during the experiment process which revealed their excellent corrosion resistance of steel rebar in the marine environment [22].

Moreover, the anodic Tafel slope (β_a), the cathodic Tafel slope (β_c) as well as the corrosion current density were determined from the Tafel extrapolation method. As shown in table 4, β_a and β_c values change in different concrete samples. The change in Tafel slope values can be used to identify the inhibition mechanism (anodic or cathodic) for carbon steel, the concentration of the electrolyte, the composition of the working electrode and charge transfer coefficient [23]. The values of the cathodic Tafel slopes, significantly unchanged in different concrete samples, which implies that its influence on the cathodic reaction did not modify the mechanism of hydrogen evolution discharge [24]. Nevertheless, the values of the slopes of the anodic Tafel lines, change in different concrete samples indicating a blockage at the anodic reaction sites, and thereby affect the anodic reaction mechanism. Furthermore, the anode Tafel slope increases in SF30MD30 sample which means a combination of SF and MD in concrete could promote the corrosion resistance of steel rebars in 5 wt% NaCl solution.

Given that electron conductive paths can be formed by addition of MD, thus the electrical resistivity and the current density of the steel rebar had decreased. Furthermore, the side effects of MD on corrosion resistance of steel reinforced concrete can be offset by adding SF, which has no remarkable effect on resistivity of MD concrete but can decrease the water absorptivity and porosity. Moreover, SF can optimize the MD dispersion in concrete. Hence, the addition of the SF and MD simultaneously helps to promote a concrete structure that reduces the absorption of water and chloride ions on the steel rebar and also can be introduced as one of the proper solutions to reduce the negative effects of adding any mineral admixtures.

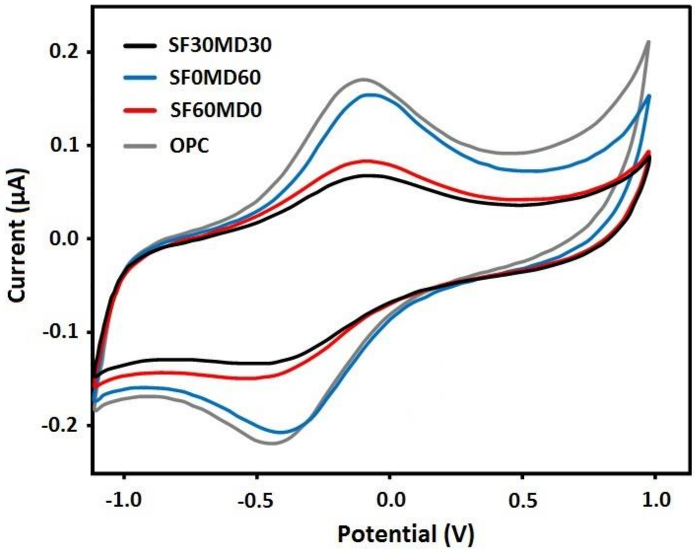

Figure 2. Cyclic voltammograms of the samples exposed to 5 wt% NaCl solution

In order to study the redox reactions and formation of the passive layer on the sample in the alkaline environment, cyclic voltammetry (CV) technique was used [25]. Figure 2 shows the cyclic voltammograms of the samples in 5 wt% NaCl solution. The anodic and cathodic peak potentials can be observed in Figure 2.

The anodic peak appeared at approximate potential of -0.15 V for all samples that is related to the following reactions from (1) to (3). It confirms the transformation from Fe^{2+} to Fe^{3+} ions and the passive layer formation on the surface of steel rebars [26]:

$$\mathrm{Fe} + 2\mathrm{O}H^{-} \leftrightarrow \mathrm{Fe\ (OH)2} + 2e^{-} \quad (1)$$

$$3\mathrm{Fe\ (OH + 2\ )}\ 2\mathrm{O}H^{-} \leftrightarrow \mathrm{Fe_3O_4} + 4\mathrm{H_2O} + 2e^{-} \quad (2)$$

$$3\mathrm{FeO} + 2\mathrm{O}H^{-} \leftrightarrow \mathrm{Fe_3O_4} + 2e^{-} \quad (3)$$

As previously reported, the current density in zero potential (i_0) can exhibit the corrosion behavior of passive layer [27]: the higher i_0 proposes poorer corrosion resistance. As shown in figure 1, SF30M30 sample reveals lower i_0, indicating lower corrosion. This reduction can be attributed to the stability of the formed passive layers on the steel surface [28]. As the potential increases up to 0.5 V, the anodic current-density suddenly decreases which can be related to the electrochemical process controlled by oxygen evolution. As shown in figure 1, the cathodic peak appeared at the potential of -0.45 V. When the potential had shifted to a more negative value, the cathodic current density increased rapidly which can be associated to the electrochemical process controlled by hydrogen evolution [29]. Furthermore, the anodic peak of SF30M30 steel rebar is lower than other samples which concludes that the mixture of MD and SF simultaneously in OPC can enhance corrosion resistance and stability of passive film on the surface of carbon steel rebar.

SF can be used as an activator in accelerating cement hydration due to its high activity. Furthermore, SF can act in cement paste as a kernel which form the small sized $Ca(OH)_2$ crystals. SF can absorb the $Ca(OH)_2$ crystals, and decrease the amount of $Ca(OH)_2$ in the concrete, resulting in the concrete becomes more resistant to adverse chemical reactions and sulfate attack [30]. The modification in the performance of reinforced concrete was significantly observed because of the use of different mineral admixture and fillers as partial replacements and it was more obvious when MD + SF replacement was used.

EIS system has been used for investigations of the corrosion resistance of carbon steel reinforced concretes prepared with different admixtures at 5 wt% NaCl solution. The Nyquist plots attained by the EIS analysis was revealed in Fig. 3. The equivalent circuit model used is indicated in Fig. 4. Where R_s is the resistance of solution. Q_c and R_c show the capacitance and the resistance element for coated concrete, respectively [31]. R_{ct} and Q_{dl} are the charge transfer resistance and the double-layer capacitance of the steel surface, respectively [32]. The determined data are indicated in Table 5.

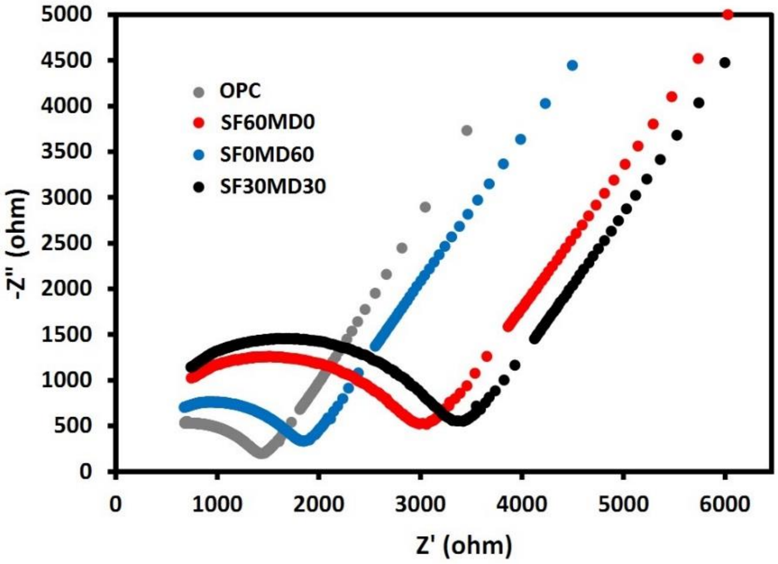

Figure 3. Nyquist plots attained from carbon steel reinforced concretes prepared with different admixtures at 5 wt% NaCl solution.

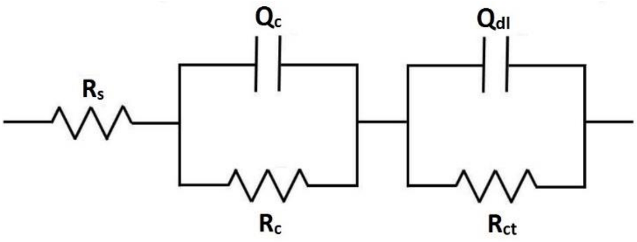

Figure 4. An equivalent circuit model

Table 5. The attained data of fitting the Nyquist diagrams for carbon steel reinforced concrete prepared with different admixtures at 5 wt% NaCl solution.

Mixtures	R_s (Ω)	R_c (Ω)	Q_c(µF cm^{-2})	R_{ct} (Ω)	Q_{dl}(µF cm^{-2})
OPC	12.4	874	5.2	1520	7.4
SF60MD0	10.7	2413	2.1	3154	3.6
SF0MD60	13.8	1759	3.8	2056	5.9
SF30MD30	11.8	2805	1.6	3540	1.8

As shown in table 5, with the appropriate replacement of SF and MD in the OPC cement, R_C increases and Q_C decreases, which exhibits an enhancement in the corrosion resistance, thickness and stability of the passive layer on the carbon steel rebar [33]. The SF have a pozzolanic reaction with the $Ca(OH)_2$ crystals and made an insoluble, dense and monolithic gel of calcium hydroxide [34]. Furthermore, the MD can form a very robust adhesion to hydrated cement because of the high surface area which leads to a better inhibition of the calcium hydroxide growth. The mineral admixtures fill the capillary pores and tiny cracks and finally shrink the cement structure. These agents increase the corrosion resistance of reinforcement steel bars in aggressive solutions [35]. Furthermore, comparing

Q_{dl} and Q_c, it was found that Q_c was lower than Q_{dl} in all samples which confirm the formation of thin passive film and the double layer at the interfaces has a high capacitive behavior [36].

The Bode diagrams attained from the EIS results are revealed in Fig. 5. Figure 5 shows that SF30M30 sample, and then SF60M0 sample indicate the best performance to inhibit the corrosion behavior in the steel reinforced concrete. These results are significantly consistent with the EIS measurement findings.

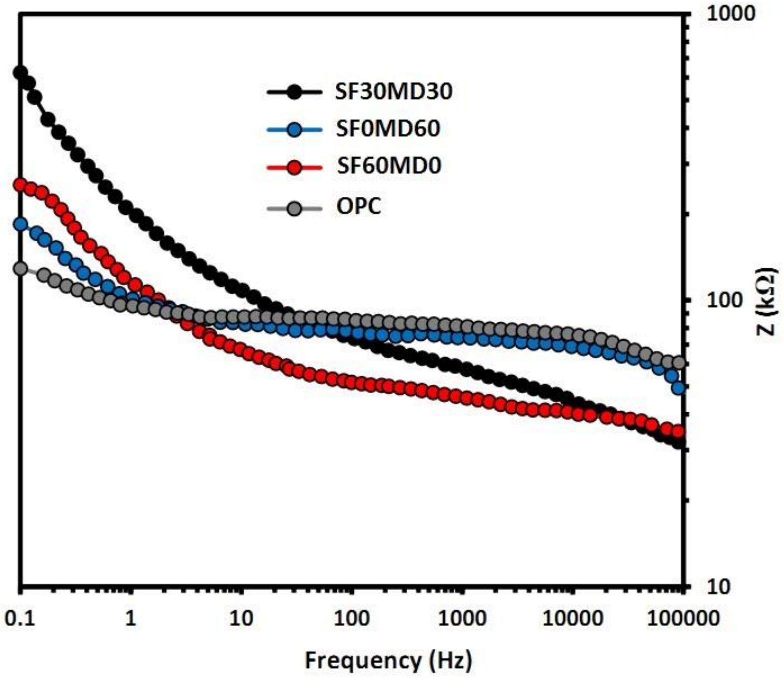

Figure 5. Bode plots of the carbon steel reinforced concrete prepared with different admixtures at 5 wt% NaCl solution.

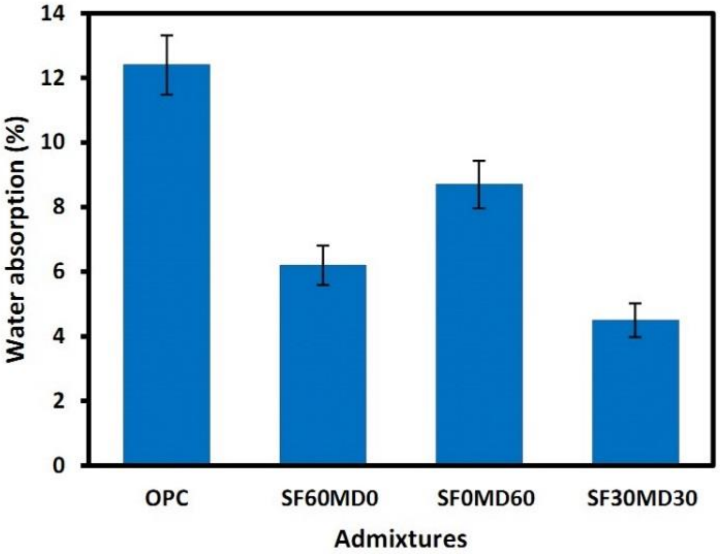

Figure 6. Water absorption of the samples after 2 months of immersing time in 5 wt% NaCl solution

Figure 6 shows the water absorption of the samples after 2 months of immersing time in 5 wt% NaCl solution. Each point of the diagram is an average of five independent measurements. As shown in figure 6, mineral admixtures had remarkable effects on water absorption of the samples, which varied between 4.5% and 12.4%. Thus, it can be presumed that the use of SF and MD as cement replacement significantly changed the water absorption of reinforced concrete. This result indicates that the water absorption has direct relation with the corrosion behavior of steel bars embedded in concrete.

Figure 7 reveals the SEM images of carbon steel surface of OPC and SF30MD30 samples after immersing in 5 wt% NaCl solution for 2 months. The surface of SF30MD30 exhibits low corrosion products and narrow pits, showing a mild pitting corrosion happened on the surface of the carbon steel rebar, which is in accordance with the results obtained from electrochemical experiments. It can be associated to the reduction of chloride ion permeability and water absorption in the concrete [37].

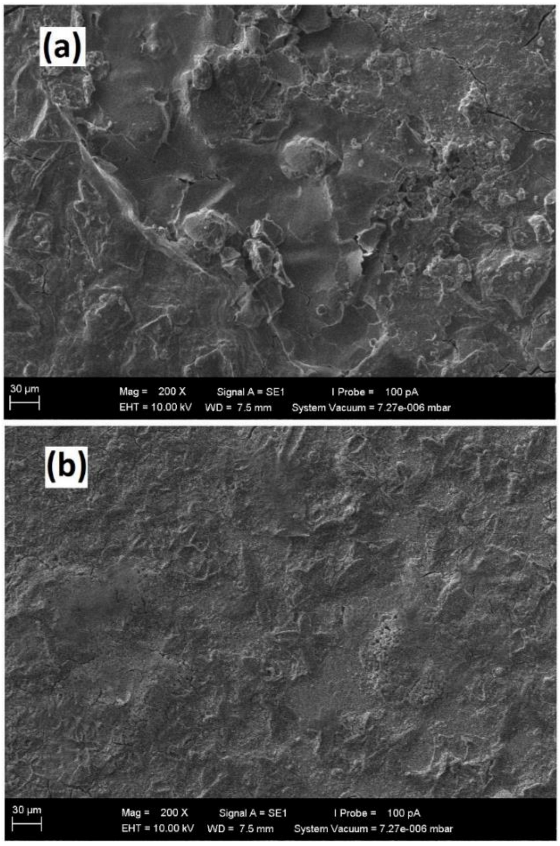

Figure 7. SEM images of carbon steel surface of OPC and SF30MD30 samples after immersing in 5 wt% NaCl solution for 2 months

4. CONCLUSION

Here, the effect of partial replacement of OPC on corrosion behavior of carbon steel reinforced concrete in 5 wt% NaCl solution were investigated. The OPC was partially replaced by combination of MD and SF admixtures. The corrosion current density of SF30M30 sample in 5 wt% NaCl environment was lower than that of the other specimens. The EIS results indicated an enhancement in the corrosion resistance, thickness and stability of the passive layer on the carbon steel rebar. The SEM image of the carbon steel surface show low corrosion products and narrow pits appeared on the surface of SF30MD30 sample which was in accordance with the results obtained from electrochemical experiments. These results indicate that partial replacement of MD and SF in OPC led to a reduction of corrosion rate and enhancement of corrosion resistance in carbon steel reinforcement because of the reduction of Cl^- ion permeability and water adsorption.

References

1. W.V. Srubar III, *Cement and Concrete Composites*, 55 (2015) 103.
2. J. Hu, G. Shaokang, C. Zhang, C. Ren, C. Wen, Z. Zeng and L. Peng, *Surface and Coatings Technology*, 203 (2009) 2017.
3. Y. Zhang, K. Bai, Z. Fu, C. Zhang, H. Zhou, L. Wang, S. Zhu, S. Guan, D. Li and J. Hu, *Applied Surface Science*, 258 (2012) 2939.
4. S.K.U. Rehman, Z. Ibrahim, S.A. Memon and M. Jameel, *Construction and building materials*, 107 (2016) 58.
5. A. Khodabakhshian, M. Ghalehnovi, J. De Brito and E.A. Shamsabadi, *Journal of cleaner production*, 170 (2018) 42.
6. E. Moreno, R. Solís-Carcaño, J. Varela-Rivera, J. Pacho-Monforte and R. Cua-Cuevas, *International Journal of Electrochemical Science*, 10 (2015) 6444.
7. T. Gupta, S. Chaudhary and R.K. Sharma, *Journal of cleaner production*, 112 (2016) 702.
8. J. Hu, C. Zhang, S. Guan, L. Wang, S. Zhu, S. Chen, J. Gao, E. Meng, S. Hou and B. Cui, *Materials Letters*, 64 (2010) 2569.
9. K. Bai, Y. Zhang, Z. Fu, C. Zhang, X. Cui, E. Meng, S. Guan and J. Hu, *Materials Letters*, 73 (2012) 59.
10. A. Ergün, *Construction and building materials*, 25 (2011) 806.
11. A.A. Aliabdo, A.E.M.A. Elmoaty and E.M. Auda, *Construction and building materials*, 50 (2014) 28.
12. G. Cao, L. Wang, Z. Fu, J. Hu, S. Guan, C. Zhang, L. Wang and S. Zhu, *Applied Surface Science*, 308 (2014) 38.
13. C. Li, S. Hu, L. Yang, J. Fan, Z. Yao, Y. Zhang, G. Shao and J. Hu, *Chemistry–An Asian Journal*, 10 (2015) 2733.
14. L. Yang, G. Yi, Y. Hou, H. Cheng, X. Luo, S.G. Pavlostathis, S. Luo and A. Wang, *Biosensors and Bioelectronics*, 141 (2019) 111444.
15. M.P. Kulakowski, F.M. Pereira and D.C.C.D. Molin, *Construction and Building Materials*, 23 (2009) 1189.
16. C. Zhu, H. Li, S. Fu, D. Du and Y. Lin, *Chemical Society Reviews*, 45 (2016) 517.
17. M.S. El-Feky, M.I. Serag, A.M. Yasien and H. Elkady, *ARPN Journal of Engineering and Applied Sciences*, 11 (2016) 13909.
18. R. Antunes, M. De Oliveira and I. Costa, *Materials and Corrosion*, 63 (2012) 586.
19. S. Kakooei, J. Rouhi, E. Mohammadpour, M. Alimanesh and A. Dehzangi, *Caspian Journal of Applied Sciences Research*, 1 (2012) 16.
20. J. Hu, C. Zhang, B. Cui, K. Bai, S. Guan, L. Wang and S. Zhu, *Applied Surface Science*, 257 (2011) 8772.
21. W. Zhao, J. Zhao, S. Zhang and J. Yang, *International Journal of Electrochemical Science* 14 (2019) 8039.
22. A.T. Yousefi, S. Ikeda, M.R. Mahmood, J. Rouhi and H.T. Yousefi, *World Applied Sciences Journal*, 17 (2012) 524.
23. Y. Zhou, S. Xu, L. Guo, S. Zhang, H. Lu, Y. Gong and F. Gao, *RSC Advances*, 5 (2015) 14804.
24. A. Ansari, M. Znini, I. Hamdani, L. Majidi, A. Bouyanzer and B. Hammouti, *Journal of Materials and Environmental Science*, 5 (2014) 81.
25. P. Shao, X. Duan, J. Xu, J. Tian, W. Shi, S. Gao, M. Xu, F. Cui and S. Wang, *Journal of hazardous materials*, 322 (2017) 532.

26. E. Volpi, A. Olietti, M. Stefanoni and S.P. Trasatti, *Journal of Electroanalytical Chemistry*, 736 (2015) 38.
27. C. Wang, S. Yang, Y. Chen, B. Wang, J. He and C. Tang, *RSC Advances*, 5 (2015) 34580.
28. X. He, F. Deng, T. Shen, L. Yang, D. Chen, J. Luo, X. Luo, X. Min and F. Wang, *Journal of colloid and interface science*, 539 (2019) 223.
29. P. Shao, L. Ding, J. Luo, Y. Luo, D. You, Q. Zhang and X. Luo, *ACS applied materials & interfaces*, 11 (2019) 29736.
30. P. Shao, J. Tian, X. Duan, Y. Yang, W. Shi, X. Luo, F. Cui, S. Luo and S. Wang, *Chemical Engineering Journal*, 359 (2019) 79.
31. K.M. Emran and H. AL-Refai, *International Journal of Electrochemical Science*, 12 (2017) 6404.
32. N. Naderi, M. Hashim, K. Saron and J. Rouhi, *Semiconductor Science and Technology*, 28 (2013) 025011.
33. S. Kakooei, H.M. Akil, A. Dolati and J. Rouhi, *Construction and Building Materials*, 35 (2012) 564.
34. J. Setina, A. Gabrene and I. Juhnevica, *Procedia Engineering*, 57 (2013) 1005.
35. J. Rouhi, C.R. Ooi, S. Mahmud and M.R. Mahmood, *Electronic Materials Letters*, 11 (2015) 957.
36. S. Pang, B. Diao and Y. Ye, *International Journal of Electrochemical Science*, 12 (2017) 5539.
37. F. Husairi, J. Rouhi, K. Eswar, A. Zainurul, M. Rusop and S. Abdullah, *Applied Physics A*, 116 (2014) 2119.